Title

Characterizing the Collagen Fiber Orientation in Pericardial Leaflets Under Mechanical Loading Conditions

Journal

Annals of Biomedical Engineering, 41(3)

ISSN

0090-6964

Authors

Alavi, S Hamed
Ruiz, Victor
Krasieva, Tatiana
et al.

Publication Date

2013-03-01

DOI

10.1007/s10439-012-0696-z

Published in final edited form as:
Ann Biomed Eng. 2013 March ; 41(3): 547–561. doi:10.1007/s10439-012-0696-z.

Characterizing the Collagen Fiber Orientation in Pericardial Leaflets Under Mechanical Loading Conditions

S. Hamed Alavi[1], **Victor Ruiz**[2], **Tatiana Krasieva**[3], **Elliot L. Botvinick**[1,3], and **Arash Kheradvar**[1]

[1]The Edwards Lifesciences Center for Advanced Cardiovascular Technology, Department of Biomedical Engineering, University of California, Irvine, Irvine, CA 92697, USA

[2]Department of Mechanical and Aerospace Engineering, University of California, San Diego, San Diego, CA, USA

[3]Beckman Laser Institute, University of California, Irvine, Irvine, CA, USA

Abstract

When implanted inside the body, bioprosthetic heart valve leaflets experience a variety of cyclic mechanical stresses such as shear stress due to blood flow when the valve is open, flexural stress due to cyclic opening and closure of the valve, and tensile stress when the valve is closed. These types of stress lead to a variety of failure modes. In either a natural valve leaflet or a processed pericardial tissue leaflet, collagen fibers reinforce the tissue and provide structural integrity such that the very thin leaflet can stand enormous loads related to cyclic pressure changes. The mechanical response of the leaflet tissue greatly depends on collagen fiber concentration, characteristics, and orientation. Thus, understating the microstructure of pericardial tissue and its response to dynamic loading is crucial for the development of more durable heart valve, and computational models to predict heart valves' behavior. In this work, we have characterized the 3D collagen fiber arrangement of bovine pericardial tissue leaflets in response to a variety of different loading conditions under Second-Harmonic Generation Microscopy. This real-time visualization method assists in better understanding of the effect of cyclic load on collagen fiber orientation in time and space.

Keywords

Bioprosthetic heart valve; Collagen fiber orientation; Second harmonic generation microscopy; Biaxial loading

INTRODUCTION

Valvular heart disease is the third most common cause of heart problems in the United States. Biological hearts valves (BHVs) made of porcine leaflets or bovine pericardium are routinely used as replacements for diseased natural valves. Their lower risks of thrombogenicity and superior hemodynamics, when compared to mechanical valves, have given these valves remarkable advantages.[33] In spite of this, BHVs do not have favorable long-term durability, primarily due to early structural failure of the leaflets.[31,44] A range of failure mechanisms have been proposed to explain observed leaflet failure.[14,23,38,40,42]

Address correspondence to Arash Kheradvar, The Edwards Lifesciences Center for Advanced Cardiovascular Technology, Department of Biomedical Engineering, University of California, Irvine, Irvine, CA 92697, USA. arashkh@uci.edu.

When implanted inside the body, heart valve leaflets experience a variety of cyclic mechanical stresses that are dynamic and complex in nature. They include: (1) *shear stress* due to blood flow when the valve is open, (2) *flexural stress* due to cyclic opening and closure of the valve, and (3) *tensile stress* when the valve is closed. These types of stress lead to a variety of failure modes, such as mechanical rupture, cyclic degradation under fatigue conditions (e.g. cyclic bending strains) and local separation in the presence of highly concentrated membrane stresses.[35,38] Other reasons for failure include loss of cusp extensibility,[1,37] and tissue calcification.[18] Structural valve deterioration[25] can also be initiated by mechanisms such as immune rejection[2,16,19] (e.g. macrophage deposition followed by collagen breakdown and calcification at the end) or atherosclerosis.[12,22] Regardless of the mode of failure, disruption of collagen fibers arranged in the extracellular matrix could be responsible for the damage.

In either a natural valve leaflet or a processed pericardial tissue leaflet, collagen fibers reinforce the tissue and provide structural integrity such that the very thin leaflet can stand enormous loads related to cyclic pressure changes. The mechanical response of the tissue greatly depends on collagen fiber concentration, characteristics, and orientation.[5,21] During loading, collagen fibers naturally align with the principal stresses applied to the thickness of the leaflet allowing the natural leaflet to properly stretch/relax due to the loading/unloading, respectively.[10] It is shown that other orientations of the collagen fibers with respect to these directions may result in fundamental structural changes in time that can affect the longevity of the valve.[9,17,41]

Thus, understating the microstructure of pericardial tissue and its response to dynamic loading is crucial for the development of more durable BHVs. In this work, we have investigated the 3D collagen fiber arrangement of bovine pericardial tissues in response to a variety of different loading conditions under Second-Harmonic Generation Microscopy. This real-time method assists in better understanding of the effect of cyclic load on collagen fiber orientation in time and space.

MATERIALS AND METHODS

Sample Preparation

Glutaraldehyde-fixed bovine pericardium (Neovasc, BC, Canada) with a thickness of 0.5 mm was cut into 3 cm × 3 cm segments to be used for multiphoton imaging. The tissue segments were hydrated prior to and during the microscopy using PBS (Gibco, Carlsbad, CA, USA).

Biaxial Mechanical Loading Device

A biaxial mechanical loading device was developed to apply uniaxial and biaxial loads under microscopy. The device included four loading grips, one stage insert, one platform, four pulleys, four tension control screws, and four force gauges (Fig. 1). The device has a modular design, which facilitates installation on different microscope stages. For this study, loading device was installed over a motorized X–Y stage on a Zeiss LSM 510 Meta multiphoton microscope (Carl Zeiss Microscopy, LLC, NY, USA). All components of the device were fabricated from light Plexiglas or polycarbonate not to weigh more than 1.5 kg in total, which is the maximal allowable load over the X–Y scanning stage. Four digital force gauges with 50 mN resolution (Mecmesin, West Sussex, UK) were used to monitor the force exerted on each grip in real time. A pulley system with thin cables couples the grips that hold the tissue segments to the connectors on the force gauges. The Plexiglas pulleys have a small ball bearing press-fitted inside to provide near-frictionless rotation.

Small grips held the tissue specimen at all four sides of the tissue segments. Tension control was achieved by placing a 10–32 screw between each grip and its corresponding force gauge, where all four screws had a hole drilled through their center to provide a passageway for the cable. Pairs of control screws were mounted orthogonal to the plate (Fig. 1A) such that screw rotation increased tension in the cable, which was displayed on the digital readout. At the beginning of each experiment, each section of the cable was pre-tensioned to reduce slack and ensure instantaneous force transfer. The magnitude of the initial pre-tension (typical value of 0.15 N) was subtracted from the final force reading for calibration. This light-weight setup provides real-time monitoring of biaxial loads applied over a thin tissue segment mounted on the stage of a high resolution nonlinear microscope.

Loading the Tissue Segments Under Microscopy

Second Harmonic Generation (SHG) images were acquired by a Zeiss LSM Meta 510 laser microscope equipped with a Ti:Sapphire (Chameleon-Ultra, Coherent) femtosecond laser source tunable from 690 to 1040 nm. SHG was excited with 900 nm light and emission was filtered from 450 to 465 nm. Experiments were performed on three bovine pericardial segments. SHG Image stacks were acquired for each segment at three centrally-located regions under four different loading conditions. The microscope field-of-view covers area of 225 μm × 225 μm of the tissue segment. Tissue segments were first measured under low initial tension to determine the collagen fiber orientation in the relaxed state. This information was also used to establish a reference to compare with the changes in fiber orientation under uniaxial and biaxial loading conditions. Next, SHG imaging was performed on the tissue segments subjected to (a) uniaxial longitudinal loading, (b) uniaxial transverse loading and (c) biaxial loading (Fig. 2a). Prior to each experiment, the direction of the fibers at the surface of tissue was obtained using multiphoton microscope. Whichever direction they had at the surface was considered as the transverse direction for loading experiment (0°). For each loading condition, 1.2 N was applied to the appropriate set of grips, considering that this load is similar to the typical loading experienced by a valve leaflet in the heart (Fig. 2b).[4,15]

Immediately after imaging the loaded samples, the grips were carefully detached and the same volume was imaged. After 10 min, the volume was imaged again to investigate the late effects of unloading on fiber orientation. The samples were kept hydrated during the experiments using PBS.

Characterizing the Collagen Fiber Orientation

Mean collagen bundle direction was extracted from SHG images (Fig. 3a) based on 2D Fourier transform analysis[24,34] using an in-house developed MATLAB code (Mathworks, MA, USA). The natural logarithm of the 2D Fast-Fourier Transform (FFT) magnitude was computed and then rearranged with frequencies shifted to bring the zero-frequency to the center of the images (Fig. 3b). The background of Fourier images was suppressed by thresholding, where the intensity threshold was defined as the mean value plus three standard deviations.[3] The frequency indices of the filtered images were extracted, plotted, and a regression line was defined through the distribution of frequencies to calculate the average orientation of the fibers (Fig. 3c). The Fourier Transform allows characterization of the frequency of light intensity oscillations for each pixel. Thus, it was possible to attain the distribution of frequencies related to the spacing of the collagen fibers. Finally, the fiber direction was extracted orthogonal to the trend of frequency distributions.

Statistical Analysis

All the data extracted from SHG images of different tissue segments were reported as mean ± SD. An unpaired Student's *t* test was performed for statistical analysis using the R

software package for Windows (Lucent Technologies Inc., Costa Mesa, CA, USA). Statistical significance was determined by p values of less than 0.05.

RESULTS

The image stacks of the bovine pericardial tissue segments for each loading condition were collected by SHG microscopy at the depths varying from 10 to 60 microns from the tissue surface. After imaging a region within the relaxed tissue, the same region was imaged again once loaded uniaxially (longitudinal and transverse) and biaxially. Then the sample was unloaded and re-imaged immediately after and after 10 min to obtain the post-loading changes, and to determine whether the fiber angles were permanently changed (viscoplastic behavior). For all the relaxed, loading and unloading conditions, angle of orientation with respect to the depth was extracted using the method described before. This was done for three samples as follows:

First Sample

Uniaxial Loading Behavior

Uniaxial Longitudinal: The SHG images of a region of tissue segment under uniaxial longitudinal loading are shown in Fig. 4. The images were acquired in depth in 10 micron increments. Images are shown for the relaxed, loading, and unloading states. In this configuration, the direction of loading was perpendicular to the conventional x-axis in x–y image plane. In the relaxed state, collagen fibers exhibit a randomly distributed pattern compared to the loaded states. Once loaded, the collagen fibers were arranged densely along the direction of loading. When the tissue segment was unloaded, the collagen fibers redistributed in a random pattern similar to the one observed in the relaxed state.

Figure 5 reports the mean orientation of angle vs. depth of imaging in all four loading states. Through the uniaxial longitudinal loading, the collagen fibers dominantly reoriented horizontally at the superficial layers, as indicated by an angle of orientation between −10 and 10° up to the depth of 20 microns. This alignment was perpendicular to the direction of the applied load. However, in deeper layers, fiber orientations were found more along the direction of the applied load. Fourier analysis indicates that at deeper layers, collagen fibers change their mean orientation under loading to align with the longitudinal load. Sudden unloading of the samples led to fiber reorientation with a mean angle similar to their relaxed state (i.e. the maximum angle difference was almost 6°). Moreover, the fibers changed their orientation in time and became even more similar to their relaxed state pattern with maximum angle difference of about 2.4°.

Uniaxial Transverse: Figure 6 displays the SHG images of a uniaxial transverse loading experiment in the same sample as Fig. 4. The figure shows the relaxed, loaded and unloaded states. The extracted collagen fiber directions are shown in Fig. 7. This experiment was performed to test whether the collagen fiber orientations depend on the direction of the uniaxial load. The transverse loading reoriented fibers by about 90° with respect to the case of uniaxial longitudinal loading. The mean fiber orientation was 60.3 ± 1.5° at 10 micron depth and between 0 and 16° at the deeper layers. The fibers arranged in-line with the direction of the applied load in deeper layers but were not exactly perpendicular to that in superficial layers. This was in contrast to the behavior found in response to uniaxial longitudinal loading. After unloading, the fibers rapidly changed their orientation with a mean angle similar to the relaxed state. The maximum angle difference between the unloaded and relaxed states was 13.9°, a value which reduced to 2.4° far along after unloading.

Biaxial Loading Behavior: The SHG images taken under biaxial loading are shown in Fig. 8. In contrast to uniaxial loading, biaxial loading did not significantly reorient fibers in the deeper layers (Fig. 9). In contrast, the fibers at the surface layers exhibited a shift in their pattern and reoriented nearly at 120° while the fibers in deeper layers arranged at almost 60°. After unloading, fibers rapidly reoriented such that the largest angle difference in fiber angle—as compared to the original relaxed state—was much greater than those observed for uniaxial loading conditions (almost 31°). However, this difference was reduced to just 2.6° late after unloading when tissue was relaxed.

Second Sample

Uniaxial Loading Behavior—The same experiment was performed for second sample. The mean fiber orientation angles in relaxed, loading and unloading states were extracted for uniaxial longitudinal (Fig. 10) and transverse (Fig. 11) loading. The fiber orientations in relaxed state were found significantly different ($p \sim 0.01$) than the first sample with the exception of the orientations at the surface, which were almost the same ($p \sim 0.62$ for the first 20 microns depth). Loading curves for both longitudinal and transverse conditions were found similar to the one shown in Fig. 5 with p values of ~0.97 and ~0.92, respectively. At superficial layers, the fibers reorient perpendicular (90°) to the direction of the applied load in longitudinal, and 65.5 ± 1.2° in transverse loadings. They were found parallel to the load at the deeper layers in both configurations. Sudden unloading of the samples resulted in rotation of the fibers to a mean angle close to their relaxed state.

Biaxial Loading Behavior—The extracted mean angles of the fibers for sample 2 are shown in Fig. 12. The fibers reoriented at 112 ± 2.4° at the surface and 50 ± 1.9° at the depth of 60 microns. The loading curve was found similar ($p \sim 0.81$) to the loading curve of the first sample. After unloading, fibers rapidly reoriented back to their relaxed state.

Third Sample

Uniaxial Loading Behavior—The extracted mean fiber angles for the sample 3 in uniaxial longitudinal and transverse loading/unloading are shown in Figs. 13 and 14, respectively. The relaxed state was found quite different than both the first and the second samples ($p \sim 0.47$ and $p \sim 0.24$, respectively). The uniaxial longitudinal loading curve was found almost similar to both loading curves shown in Fig. 5 for the first sample and Fig. 10 for the second sample ($p \sim 0.82$ and $p \sim 0.79$, respectively). The p values for uniaxial transverse loading were $p \sim 0.92$ for sample 1 and $p \sim 0.85$ for sample 2. After unloading no viscoplastic behavior was observed.

Biaxial Loading Behavior—The extracted mean angles of the fibers for sample 3 shows that the fibers reoriented at 129 ± 3.5° at the surface and 45 ± 1.2° at the depth of 60 microns (Fig. 15). The biaxial loading curve provided a similar response as the loading curves of the previous samples ($p \sim 0.93$ and $p \sim 0.77$, respectively). Sudden and delayed unloading, reoriented the fibers close to their relaxed state.

DISCUSSION

Several optical methods (e.g. Small Angle Light Scattering[11,26,27] and reflection confocal microscopy[39]) have been developed for estimating fiber orientation within a valve leaflet that do not require chemical fixation, sectioning or dehydration. However, each entails some limitation. We chose to implement SHG microscopy, a widely used method for imaging collagenous biological tissue such as heart valve leaflets,[29,30] that does not require use of exogenous molecular probes. SHG is a nonlinear mode of microscopy based on coherent second-order nonlinear scattering, which may occur when a non-centrosymmetric molecular

structure is illuminated by light sources such as a Near Infrared (NIR) femtosecond-pulsed coherent laser. The molecules will emit light at half the wavelength of the laser.[24] Collagen type I has a highly crystalline triple-helix structure effective at SHG conversion.[7,8,13] Since the intensity of SHG signals is modulated by laser polarization angle (for linear polarization), fiber orientation can be determined from an image stack representing linear polarization scanned by an actuated waveplate.[43] Alternatively, fiber orientation can be extracted from Fourier analysis of images, as in Fig. 3. When this technique is coupled with mechanical stimulation,[6,36] further information regarding the behavior of tissues in configurations other than the stress-free state, typically in dynamic loading and hysteresis, can be obtained. In this study, “dynamic” or “cyclic” means that we have the information for unloading as well as the loading conditions. While the macroscopic mechanical response of the heart valve tissue under the cyclic load has been studied before, we tried in this study to visualize how a uniaxial or biaxial load/unload can change the orientation of the fibers at microscopic scale during and after applying a load.

Heart Valve Biomechanics

The composite loads experienced by heart valve leaflets can be decoupled into in-plane stretch (i.e. shear, tensile stresses) and flexural deformation modes.[20,28] When the heart valve is open, the dominant loads applied to the leaflets are surface shear stresses due to passage of blood flow. Once the valve is closed the tensile stresses due the high pressure in the cardiac chambers will be of more importance. The valve leaflets experience significant bending stresses while transitioning between open and close states. Thus, a durable heart valve leaflet must be resilient to these rapidly changing internal stresses. This resilience should originate from type and alignment of the leaflet’s ultrastructure.

Despite the large number of studies emphasizing the role of collagen fiber orientation in anisotropic mechanical properties of pericardial tissue, little is yet known about the effect of loading on temporal and spatial variations of collagen fiber orientation. In this study, we have characterized the collagen fiber orientation in bovine pericardial tissue leaflets during different loading conditions by implementing Fourier analysis of SHG image stacks. The specimens were analyzed during relaxed, loading and unloading states using our novel microscope-stage biaxial tensile tester.

According to the current convention developed by Billiar and Sacks,[5] We considered the load applied in direction of the leaflet symmetry line as radial stress and the one perpendicular to it in-plane as circumferential. Through these definitions, we were able to imitate the surface shear and tensile stresses as longitudinal and transverse stresses (or vice versa depending on the orientation of the tissue segment), in our biaxial tensile tester. Based on the data provided by Sacks and Yoganathan,[28] previous studies showed that in a natural heart valve the radial strain and strain rates are nearly three times greater than the circumferential ones that implies higher extensibility in the radial direction. This phenomenon indicates that the leaflets damp the shear stress by means of radial elongation of the fibers when the valve is open. Efficient radial elongation requires that the fibers transform from their wavy to an aligned configuration and reorient in the direction of blood flow. With increasing the stress to a certain amount, the fibers become highly aligned with the direction of flow and the valve becomes stiffer.[5]

Uniform biaxial loading is a good model of the valve’s loading conditions when it is closed. Here, the radial and circumferential stresses are equivalent to longitudinal and transverse stresses (or vice versa) as implemented in our experiment. From loading standpoint, the valve’s behavior when it is open can be imitated by a uniaxial longitudinal or transverse loading situation while its closure is comparable to the biaxial loading. Our data suggests that the superficial collagen fibers in fixed bovine pericardial tissues (i.e. the fibers between

the surface and 20 microns depth) under a uniaxial radial loading condition orient perpendicular to the load direction. This configuration gives the surface layers enough compliance and can be of more importance in *in vivo* situation so that the flow-related shear stress would not damage the tissue surface. Deeper layers of tissue, which generally define the mechanical resilience, have fibers that align parallel to the direction of the load. This will potentially assist in damping the tensile stress and make the tissue stiffer. Observing different effects at variable depths should be due to the (1) heterogenic structure of the tissues; as the extracellular matrix and particularly collagen fibers are not homogeneous, and (2) the viscoelastic properties of the material. In biaxial loading, which replicates the valve's closure condition, the fibers align in the middle of two principal stresses; more specifically, they tend to mimic their stress-free condition at about 60°. This is potentially due to the anisotropic mechanical properties of the tissue in radial and circumferential directions that leads to a higher stiffness in one direction. As a result, the fibers align in an angle closer to that direction (i.e. they align in 60° instead of 45°). This phenomenon is expected to happen during the valve closure when the collagen fibers are loaded and allow the valve closure to progress smoothly.

The flexural loading situation could not be modeled with the current setup due to lack of bending load in the tissue. However, If we consider the leaflet as a shell, the mechanical behavior of its each element can be decomposed and modeled based on uniaxial loading and a moment applied to that element where the magnitude of this moment is varied depending on the location of the element (e.g. very low at the basal attachment). In this study, since the size of each captured segment (225 × 225 μm) is negligible compared to the size of the leaflet, the obtained collagen map for each segment should be considered as one element on the leaflet tissue. Moreover, the obtained results in this study are independent from the situation in which bending is added. As a result bending loading may not play an important role on mapping the collagen fibers using the presented technique.

Applications in Heart Valve Development

Considering the fact that long-term durability of tissue valves are highly dependent on the quality of their extracellular matrix, especially collagen fibers,[32] the data presented here can be utilized in design and fabrication process of the pericardial valve. The current process on fabrication of pericardial bioprosthetic valves does not consider the direction of the tissue fibers with respect to the flow. This may be a reason for the heterogeneity observed in longevity of these valves. The two different configurations of uniaxial loading (i.e. longitudinal and transverse) showed a slightly different response in their collagen reorientation. In surface layers, they reorient almost perpendicular to the load in the longitudinal situation while they orient at 60° to the load (and not 90°) in the transverse state. Moreover, the disruption of collagen fibers orientation is much lower in longitudinal loading configuration than the transverse state. It seems that the tissue will have a better response (in case of fiber orientation) to flow-related shear stresses in a specified uniaxial direction (longitudinal here). During sewing or fabrication of the valve, if this specified direction (i.e. the direction normal to the direction of the fibers at the surface of the tissue in relaxed states) is selected as the radial direction of the leaflets, a better response to load could be expected due to proper realignment of the fibers, which may result in enhanced durability.

Our experimental results indicated that the orientation of the fibers depends on the location of imaged segments within the thickness of tissue, and in fact, ability to image deeper layers may result in further information regarding the collagen fibers. We also observed that the configuration of the fibers in glutaraldehyde-fixed bovine pericardial tissues is very similar

to the ones seen in native valve leaflet tissues. This justifies the durability and popularity of this type of tissue for heart valve purposes.

Studying the tissue segments after unloading of the samples for all loading regimes suggest that the viscoplastic behavior in this type of tissue is quite negligible since the curves of unloading become highly aligned with relaxed state at later times. Although there was no mean difference in orientation but the bundling effect of the fibers may not be reversible.

In Fig. 16 the superposition of fiber orientation in uniaxial longitudinal and transverse loading states of all samples were compared to their biaxial loaded condition. The figure confirms that no linear correlation between the two charts exists for all of the samples and they both display linearly independent responses to the load. Therefore, it can be concluded that the coupling effect in biaxial state, which make the valve's response different from uniaxial loading condition, is more complex. Finding this nonlinear relationship helps to better characterize the mechanical response of the tissue, and requires a statistically significant sample size to draw a meaningful correlation.

Limitations

There may be a minor shift in some SHG images since the loading and unloading processes might very slightly displaced the tissue segments regardless of our efforts to keep the location and orientation of tissue segment the same all over the experiment. Besides that, multiphoton imaging techniques such as SHG have limited depth of penetration within turbid tissues such as cross-linked bovine pericardium (~600 μm thick) and cannot optically section the entire thickness. To address this, we plan to use *optical clearing* technique to image collagen structures 300 μm deep (or half the pericardial thickness) in pericardial tissue.

In this study we compared the fiber orientation of three tissue segments. However, more samples are required to draw a statistically significant conclusion with respect to the effect loadings on fiber orientation. This is particularly true with respect to *in vivo* situations. Bending forces seem to be an important factor that may influence valve durability, and adding a bending moment to the entire tissue—when reconstructed—will elucidate further information. This bending moment can also be computationally applied to the results. Additionally, characterizing the collagen fiber orientation under repeated loading and unloading conditions may elucidate further information regarding durability of the tissue leaflets.

Acknowledgments

This work is supported by a Coulter Translational Research Award (CTRA) by the Wallace H. Coulter Foundation that was provided to Dr. Kheradvar. This research was also made possible in part through access to the Laser Microbeam and Medical Program (LAMMP), an NIH/NIBIB Biomedical Technology Center, P41EB05890.

REFERENCES

1. Adamczyk MM, Vesely I. Biaxial strain distributions in explanted porcine bioprosthetic valves. J. Heart Valve Dis. 2002; 11:688–695. [PubMed: 12358406]
2. Alavi SH, Liu WF, Kheradvar A. Inflammatory response assessment of a hybrid tissue-engineered heart valve leaflet. Ann. Biomed. Eng. 2012 (in press).
3. Ambekar Ramachandra Rao, R.; Mehta, MR.; Leithem, S.; Toussaint, KC, Jr. Biomedical Optics. Optical Society of America; 2010. Fourier transform-second-harmonic generation imaging of collagen fibers in biological tissues.
4. Bellhouse B. Velocity pressure distributions in the aortic valve. J. Fluid Mech. 1969; 37:587–600.

5. Billiar KL, Sacks MS. Biaxial mechanical properties of the native and glutaraldehyde-treated aortic valve cusp: part II—a structural constitutive model. J. Biomech. Eng. 2000; 122:327. [PubMed: 11036555]
6. Boulesteix T, Pena AM, Pages N, Godeau G, Sauviat MP, Beaurepaire E, Schanne-Klein MC. Micrometer scale ex vivo multiphoton imaging of unstained arterial wall structure. Cytometry Part A. 2006; 69:20–26.
7. Chen J, Lee A, Zhao J, Wang H, Lui H, McLean DI, Zeng H. Spectroscopic characterization and microscopic imaging of extracted and in situ cutaneous collagen and elastic tissue components under two-photon excitation. Skin Res. Technol. 2009; 15:418–426. [PubMed: 19832952]
8. Cox G, Kable E, Jones A, Fraser I, Manconi F, Gorrell MD. 3-dimensional imaging of collagen using second harmonic generation. J. Struct. Biol. 2003; 141:53–62. [PubMed: 12576020]
9. Driessen NJB, Bouten CVC, Baaijens FPT. Improved prediction of the collagen fiber architecture in the aortic heart valve. J. Biomech. Eng. 2005; 127:329–336. [PubMed: 15971711]
10. Driessen N, Peters G, Huyghe J, Bouten C, Baaijens F. Remodelling of continuously distributed collagen fibres in soft connective tissues. J. Biomech. 2003; 36:1151–1158. [PubMed: 12831741]
11. Engelmayr GC Jr, Papworth GD, Watkins SC, Mayer JE Jr, Sacks MS. Guidance of engineered tissue collagen orientation by large-scale scaffold microstructures. J. Biomech. 2006; 39:1819–1831. [PubMed: 16043186]
12. Farivar RS, Cohn LH. Hypercholesterolemia is a risk factor for bioprosthetic valve calcification and explantation. J. Thorac. Cardiovasc. Surg. 2003; 126:969. [PubMed: 14566234]
13. Georgiou E, Theodossiou T, Hovhannisyan V, Politopoulos K, Rapti GS, Yova D. Second and third optical harmonic generation in type I collagen, by nanosecond laser irradiation, over a broad spectral region. Opt. Commun. 2000; 176:253–260.
14. Gloeckner DC, Billiar KL, Sacks MS. Effects of mechanical fatigue on the bending properties of the porcine bioprosthetic heart valve. ASAIO J. 1999; 45:59–63. [PubMed: 9952009]
15. Grande KJ, Cochran RP, Reinhall PG, Kunzelman KS. Stress variations in the human aortic root and valve: the role of anatomic asymmetry. Ann. Biomed. Eng. 1998; 26:534–545. [PubMed: 9662146]
16. Human P, Zilla P. The possible role of immune responses in bioprosthetic heart valve failure. J. Heart Valve Dis. 2001; 10:460–466. [PubMed: 11499591]
17. Kheradvar A, Falahatpisheh A. The effects of dynamic saddle annulus and leaflet length on transmitral flow pattern and leaflet stress of a bileaflet bioprosthetic mitral valve. J. Heart Valve Dis. 2012; 21:225–233. [PubMed: 22645859]
18. Lawford PV, Black MM, Drupy PJ. The in vivo durability of bioprosthetic heart valves: mores of failure observed in explanted valves. Eng. Med. 1987; 16:95–103. [PubMed: 3622894]
19. Manji RA, Zhu LF, Nijjar NK, Rayner DC, Korbutt GS, Churchill TA, Rajotte RV, Koshal A, Ross DB. Glutaraldehyde-fixed bioprosthetic heart valve conduits calcify and fail from xenograft rejection. Circulation. 2006; 114:318–327. [PubMed: 16831988]
20. May-Newman K, Lam C, Yin FCP. A hyperelastic constitutive law for aortic valve tissue. J. Biomech. Eng. 2009:131.
21. Mol A, Driessen NJB, Rutten MCM, Hoerstrup SP, Bouten CVC, Baaijens FPT. Tissue engineering of human heart valve leaflets: a novel bioreactor for a strain-based conditioning approach. Ann. Biomed. Eng. 2005; 33:1778–1788. [PubMed: 16389526]
22. Nollert G, Miksch J, Kreuzer E, Reichart B. Risk factors for atherosclerosis and the degeneration of pericardial valves after aortic valve replacement. J. Thorac. Cardiovasc. Surg. 2003; 126:965. [PubMed: 14566233]
23. Pibarot P, Dumesnil JG. Prosthetic heart valves. Circulation. 2009; 119:1034–1048. [PubMed: 19237674]
24. Rao RA, Mehta MR, Toussaint KC Jr. Fourier transform-second-harmonic generation imaging of biological tissues. Opt. Express. 2009; 17:14534–14542. [PubMed: 19687932]
25. Ruel M, Kulik A, Rubens FD, Bédard P, Masters RG, Pipe AL, Mesana TG. Late incidence and determinants of reoperation in patients with prosthetic heart valves. Eur. J. Cardiothorac. Surg. 2004; 25:364–370. [PubMed: 15019662]

26. Sacks MS, Chuong CJ, More R. Collagen fiber architecture of bovine pericardium. ASAIO J. 1994; 40:PM632–PM637.
27. Sacks MS, Smith DB, Hiester ED. A small angle light scattering device for planar connective tissue micro-structural analysis. Ann. Biomed. Eng. 1997; 25:678–689. [PubMed: 9236980]
28. Sacks MS, Yoganathan AP. Heart valve function: a biomechanical perspective. Philos. Trans. R. Soc. B Biol. Sci. 2007; 362:1369–1391.
29. Schenke-Layland K. Non-invasive multiphoton imaging of extracellular matrix structures. J. Biophotonics. 2008; 1:451–462. [PubMed: 19343671]
30. Schenke-Layland K, Madershahian N, Riemann I, Starcher B, Halbhuber KJ, Konig K, Stock UA. Impact of cryopreservation on extracellular matrix structures of heart valve leaflets. Ann. Thorac. Surg. 2006; 81:918–926. [PubMed: 16488695]
31. Schoen F, Levy R. Pathology of substitute heart valves. J. Cardiac Surg. 1994; 9:222–227.
32. Schoen FJ, Levy RJ. Tissue heart valves: current challenges and future research perspectives. J. Biomed. Mater. Res. 1999; 47:439–465. [PubMed: 10497280]
33. Senthilnathan V, Treasure T, Grunkemeier G, Starr A. Heart valves: which is the best choice? Cardiovasc. Surg. 1999; 7:393–397. [PubMed: 10430519]
34. Sivaguru M, Durgam S, Ambekar R, Luedtke D, Fried G, Stewart A, Toussaint KC Jr. Quantitative analysis of collagen fiber organization in injured tendons using Fourier transform-second harmonic generation imaging. Opt. Express. 2010; 18:24983–24993. [PubMed: 21164843]
35. Thubrikar M, Deck J, Aouad J, Nolan S. Role of mechanical stress in calcification of aortic bioprosthetic valves. J. Thorac. Cardiovasc. Surg. 1983; 86:115–125. [PubMed: 6865456]
36. Timmins LH, Wu Q, Yeh AT, Moore JE, Greenwald SE. Structural inhomogeneity and fiber orientation in the inner arterial media. Am J Physiol Heart Circ Physiol. 2010; 298:H1537–H1545. [PubMed: 20173046]
37. Vesely I, Barber JE, Ratliff NB. Tissue damage and calcification may be independent mechanisms of bioprosthetic heart valve failure. J. Heart Valve Dis. 2001; 10:471–477. [PubMed: 11499593]
38. Vesely I, Bougher D, Song T. Tissue buckling as a mechanism of bioprosthetic valve failure. Ann. Thorac. Surg. 1988; 46:302–308. [PubMed: 3137903]
39. Voytik-Harbin SL, Roeder BA, Sturgis JE, Kokini K, Robinson JP. Simultaneous mechanical loading and confocal reflection microscopy for three-dimensional microbiomechanical analysis of biomaterials and tissue constructs. Microsc. Microanal. 2003; 9:74–85. [PubMed: 12597789]
40. Vyavahare N, Ogle M, Schoen FJ, Zand R, Gloeckner DC, Sacks MS, Levy RJ. Mechanisms of bioprosthetic heart valve failure: fatigue causes collagen denaturation and glycosaminoglycan loss. J. Biomed. Mater. Res. 1999; 46:44–50. [PubMed: 10357134]
41. Weinberg EJ, Kaazempur Mofrad MR. A finite shell element for heart mitral valve leaflet mechanics, with large deformations and 3D constitutive material model. J. Biomech. 2007; 40:705–711. [PubMed: 16574127]
42. Wheatly DH, Fisher J, Reece IJ, Spyt T, Breeze P. Primary tissue failure in pericardial heart valves. J. Thorac. Cardiovasc. Surg. 1999; 94:367.
43. Yasui T, Tohno Y, Araki T. Determination of collagen fiber orientation in human tissue by use of polarization measurement of molecular second-harmonic-generation light. Appl. Opt. 2004; 43:2861–2867. [PubMed: 15143809]
44. Yoganathan, A. The Biomedical Engineering Handbook. Boca Raton: CRC Press; 1995. Cardiac valve prostheses.

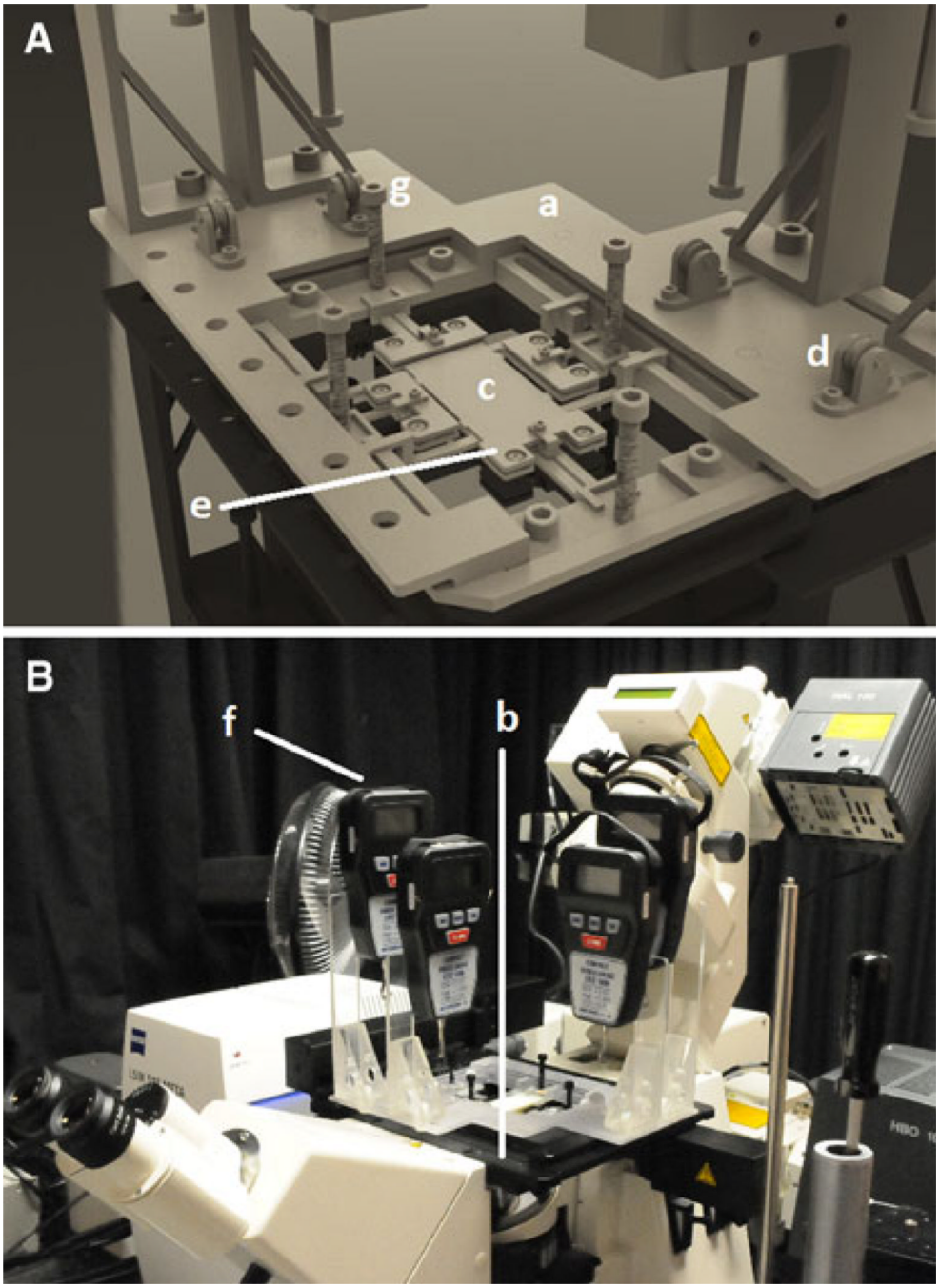

FIGURE 1.

The custom made biaxial testing machine. (A) A rectangular stage insert (a) with four chamfered corners was built to fit into the X–Y scanning stage (b). The platform geometry (c) was designed so that a pulley system (d) would allow force transfer from the grips (e), located on each side of the specimen, to the force gauges (f), located on the outskirts of the platform. A 10–32 screw (g) was considered between each grip and its corresponding force gauge to achieve tension control; (B) the whole view of the loading-imaging experimental system used in this study.

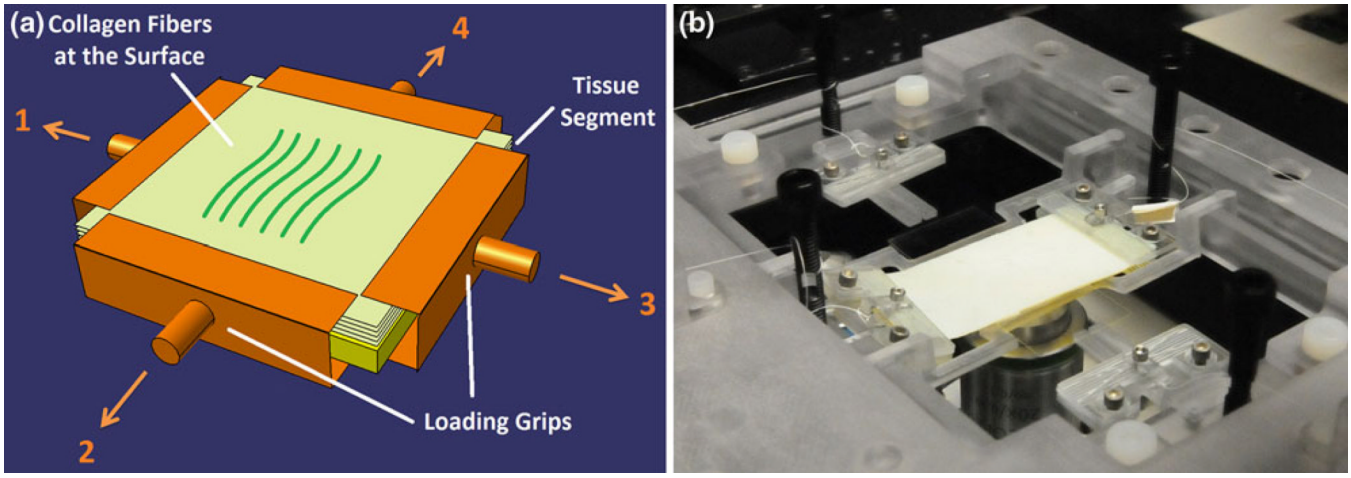

FIGURE 2.

(a) Schematic representation of different loading configurations of the pericardial tissue loading-imaging experiment. The uniaxial longitudinal experiments were performed by applying the loads 1 and 3. The loads 2 and 4 were applied for uniaxial transverse experiments while all the loads were considered for biaxial experiment. The orientation of the fibers at the surface was considered the transverse direction in this experiment. Each load magnitude was 1.2 N and the tissue segment was 3 cm by 3 cm. The imaging was repeated at three centrally-located spots in each situation; (b) device stage insert during a sample device run. It shows how two grips were attached to a tissue segment to exert uniaxial tension on it.

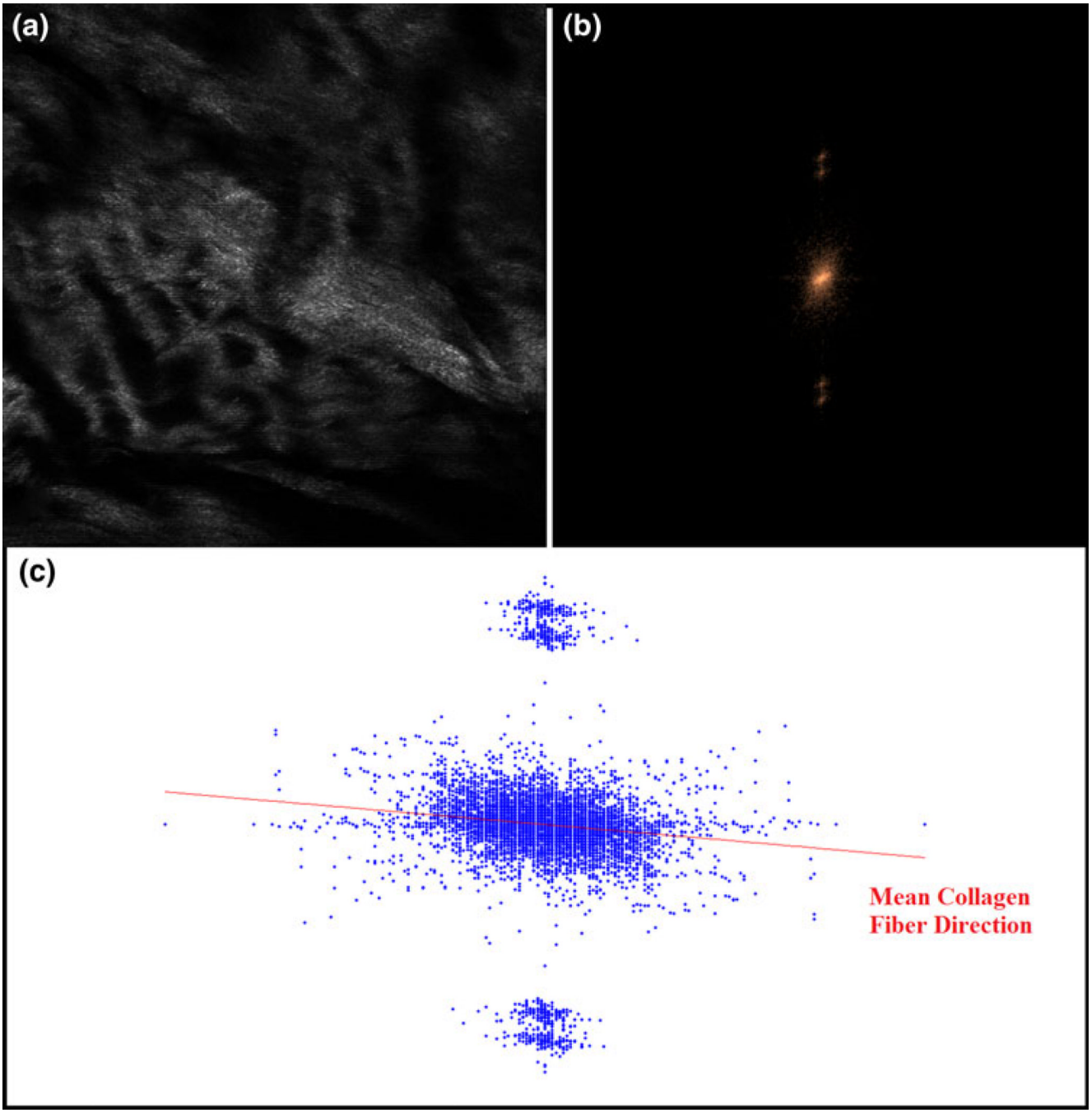

FIGURE 3.

Fourier analysis measures average fiber orientation. (a) A sample SHG collagen image excited at 900 nm with a Zeiss 510 Meta multiphoton microscopy; (b) and (c) Fourier transform images reveal mean fiber direction. These images are the natural logarithm of the FFT magnitudes (computed in Matlab with FFT2) with frequencies shifted to bring the zero-frequency to the center of the image. After segmenting the image by k-means clustering, linear regression was performed to determine the orientation of the long axis of the central bright region in each transform. The mean fiber direction is rotated 90° from that axis.

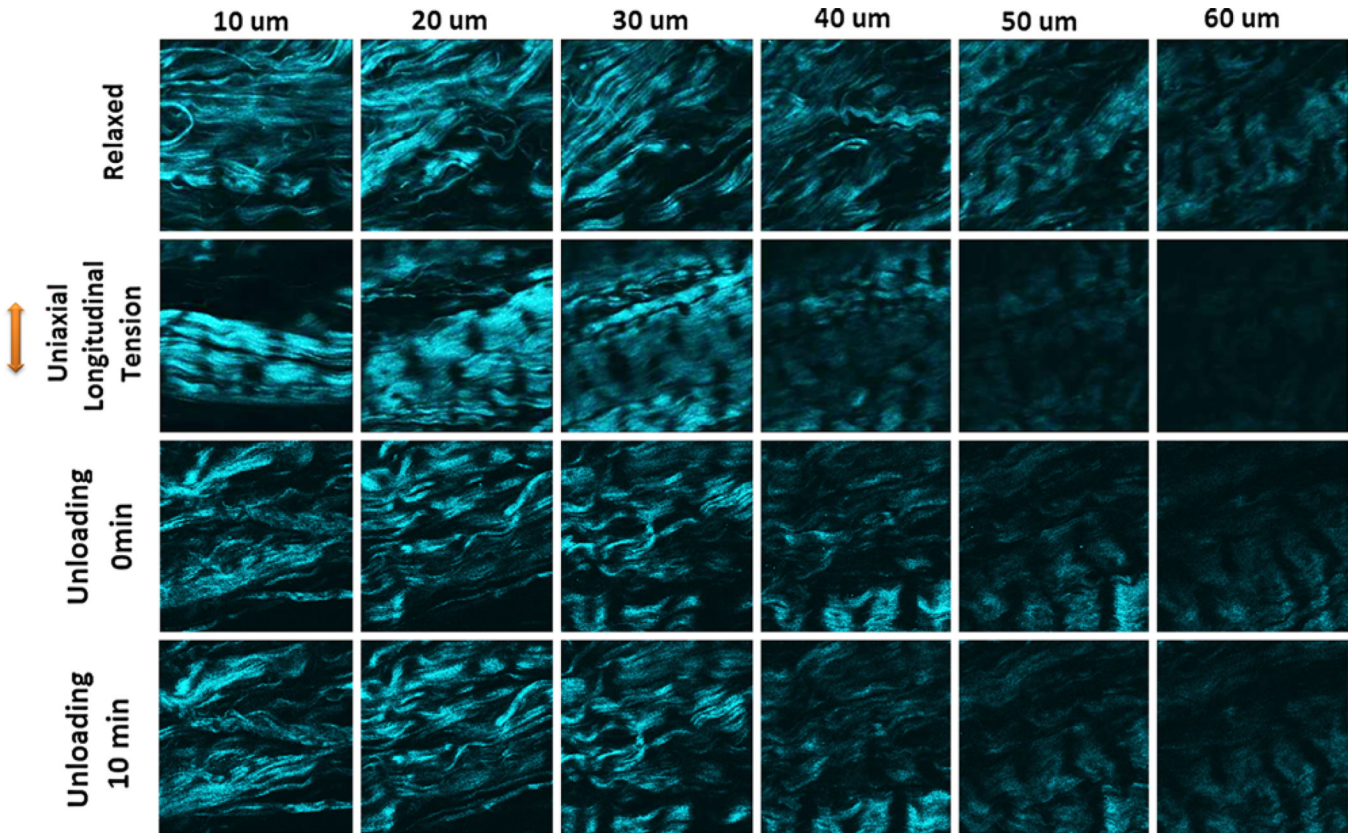

FIGURE 4.

Collagen fiber distributions for the first sample sheet of bovine pericardium taken by loading-imaging technique described. They show the change in the orientation of collagen fibers for relaxed, longitudinal loading and unloading states every 10 μm for up to 60 μm depth. The unloading images were taken in two different steps; simultaneously after unloading and 10 min after unloading. As can be seen collagen fibers orientation change profoundly during loading condition and then reorient at the same position in their relaxed state after unloading. The angle of loading is 90° with respect to the conventional x axis.

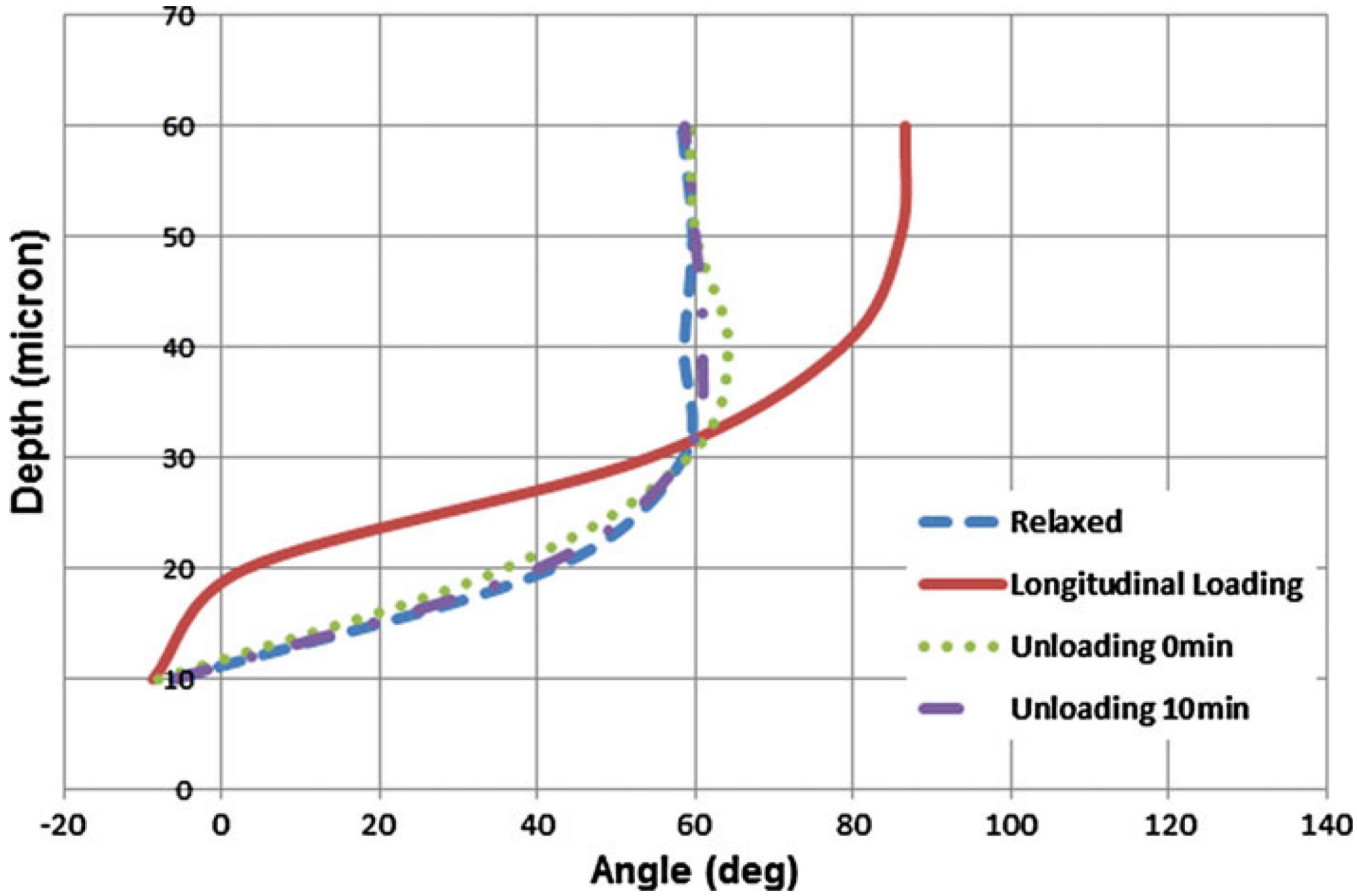

FIGURE 5.

Comparison of collagen fiber orientation in relaxed, loaded and unloaded (right after loading and 10 min after loading) states of the first bovine pericardial sheet. Uniaxial longitudinal loading state shows that fibers are almost perpendicular to force at the surface and in-line with the force in deeper layers.

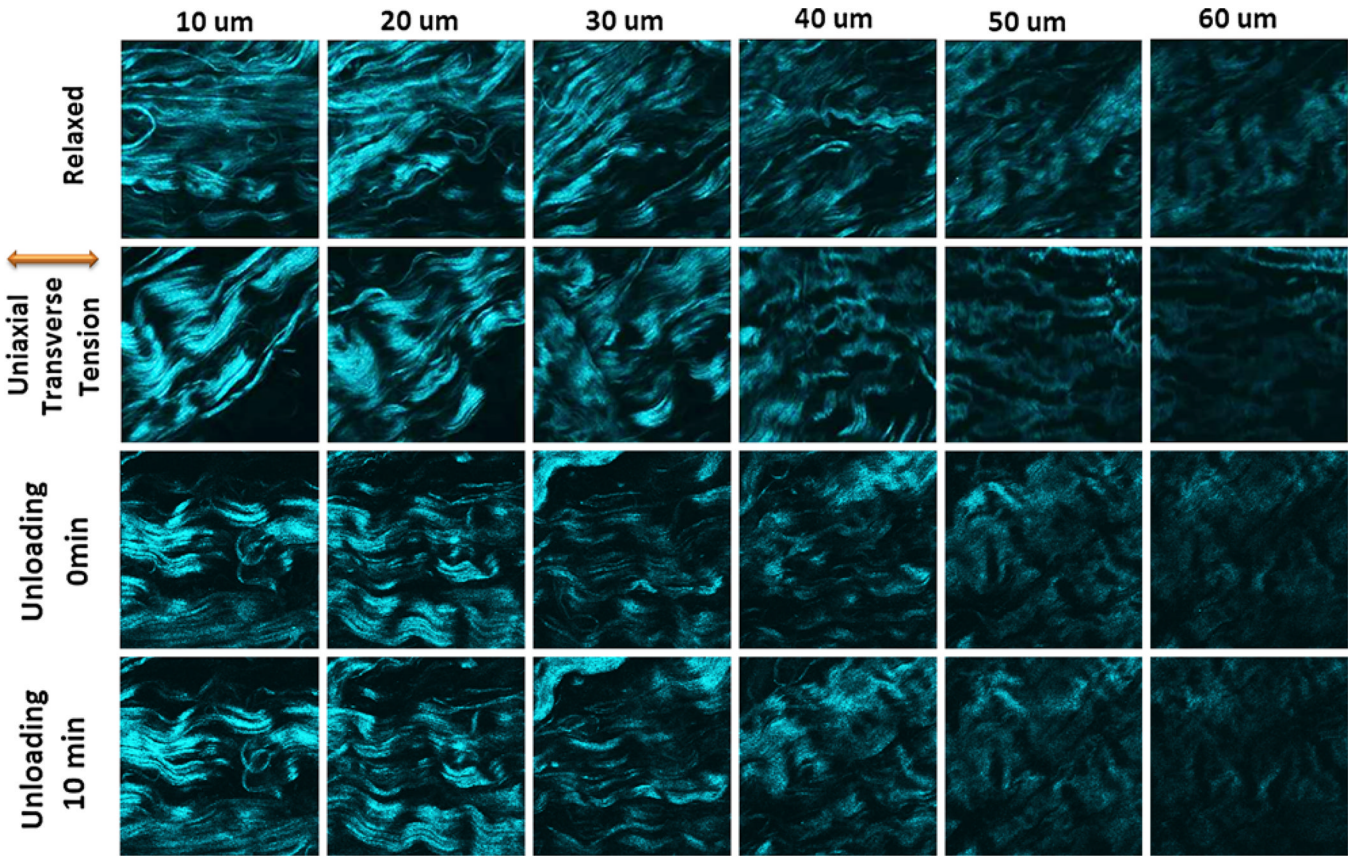

FIGURE 6.

Collagen fiber distributions for the first sample sheet of bovine pericardium taken by loading-imaging technique described. They show the change in the orientation of collagen fibers for relaxed, transverse loading and unloading states every 10 μm for up to 60 μm depth. The unloading images were taken in two different steps; simultaneously after unloading and 10 min after unloading. As can be seen collagen fibers orientation change differently than the longitudinal situation but they have the similar behavior after unloading. The angle of loading is 0° with respect to the conventional x axis.

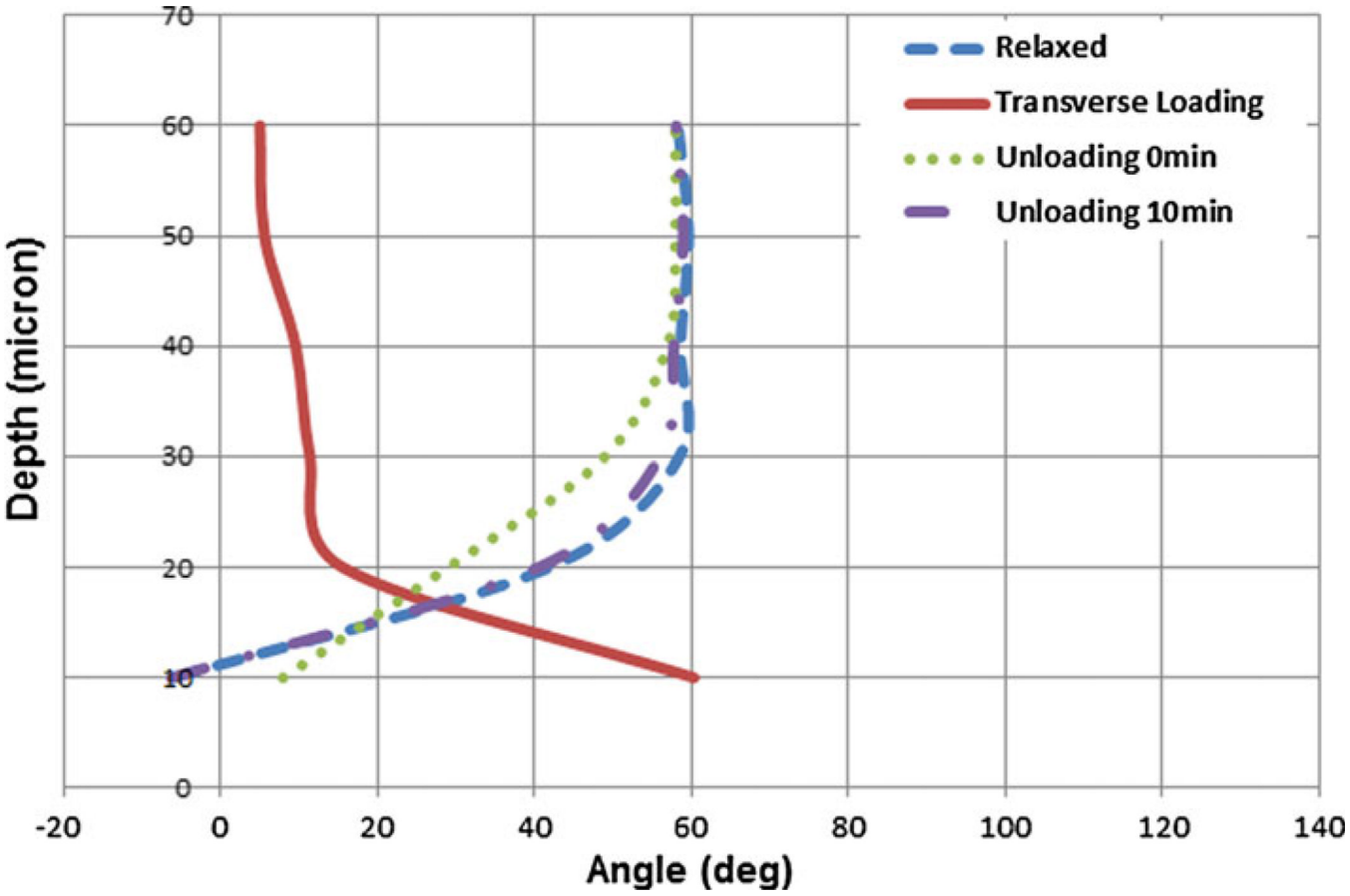

FIGURE 7.
Comparison of collagen fiber orientation in relaxed, loaded and unloaded (right after loading and 10 min after loading) states of the first bovine pericardial sheet. Uniaxial transverse loading state shows the same phenomena as the uniaxial longitudinal loading but with almost 90° angle shift in deeper layers.

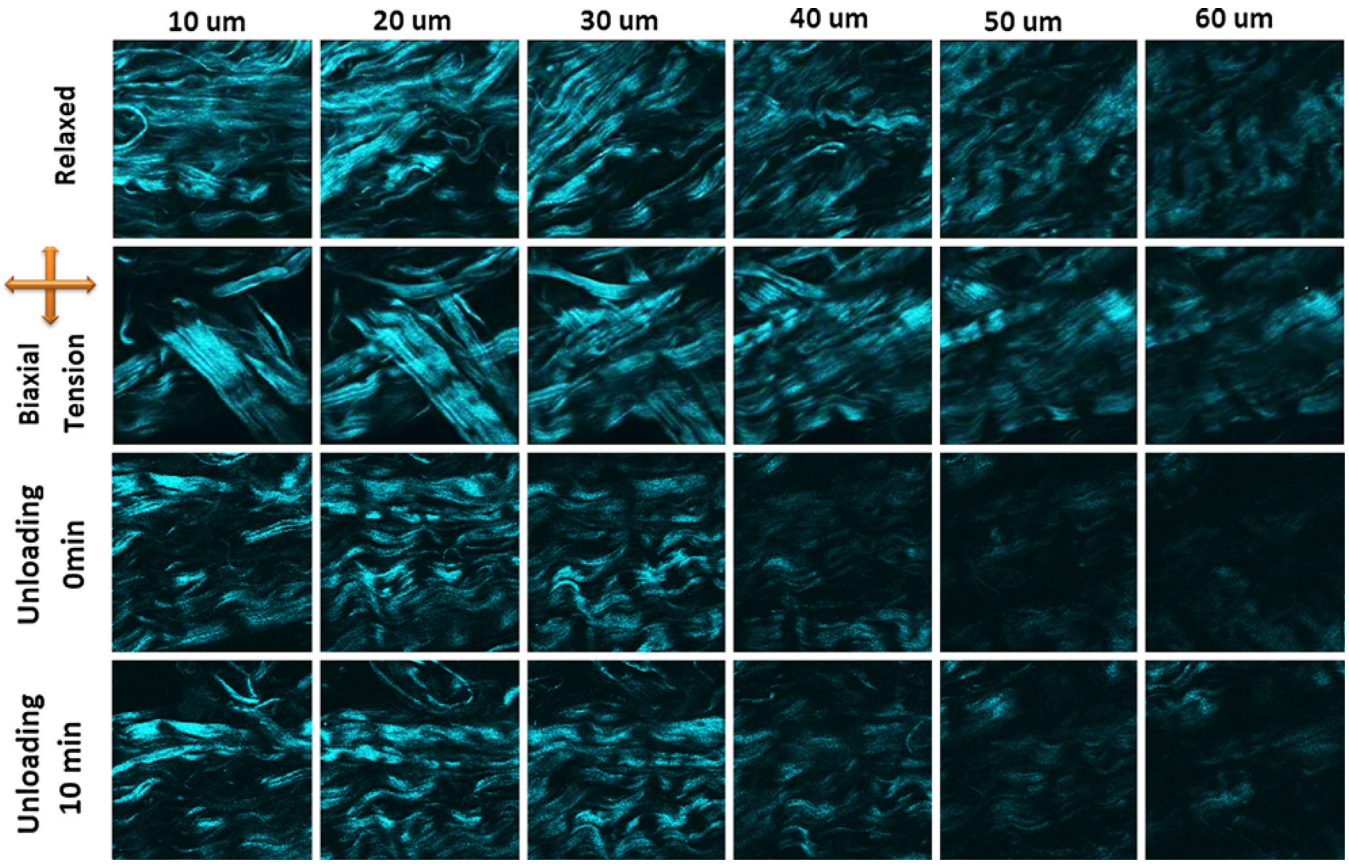

FIGURE 8.

Collagen fiber distributions for the first sample sheet of bovine pericardium taken by loading-imaging technique described. They show the change in the orientation of collagen fibers for relaxed, biaxial loading and unloading states every 10 μm for up to 60 μm depth. The unloading images were taken in two different steps; simultaneously after unloading and 10 min after unloading. As can be seen collagen fibers orientation is no longer in the direction of principal stresses while they show a similar behavior to the uniaxial ones after unloading.

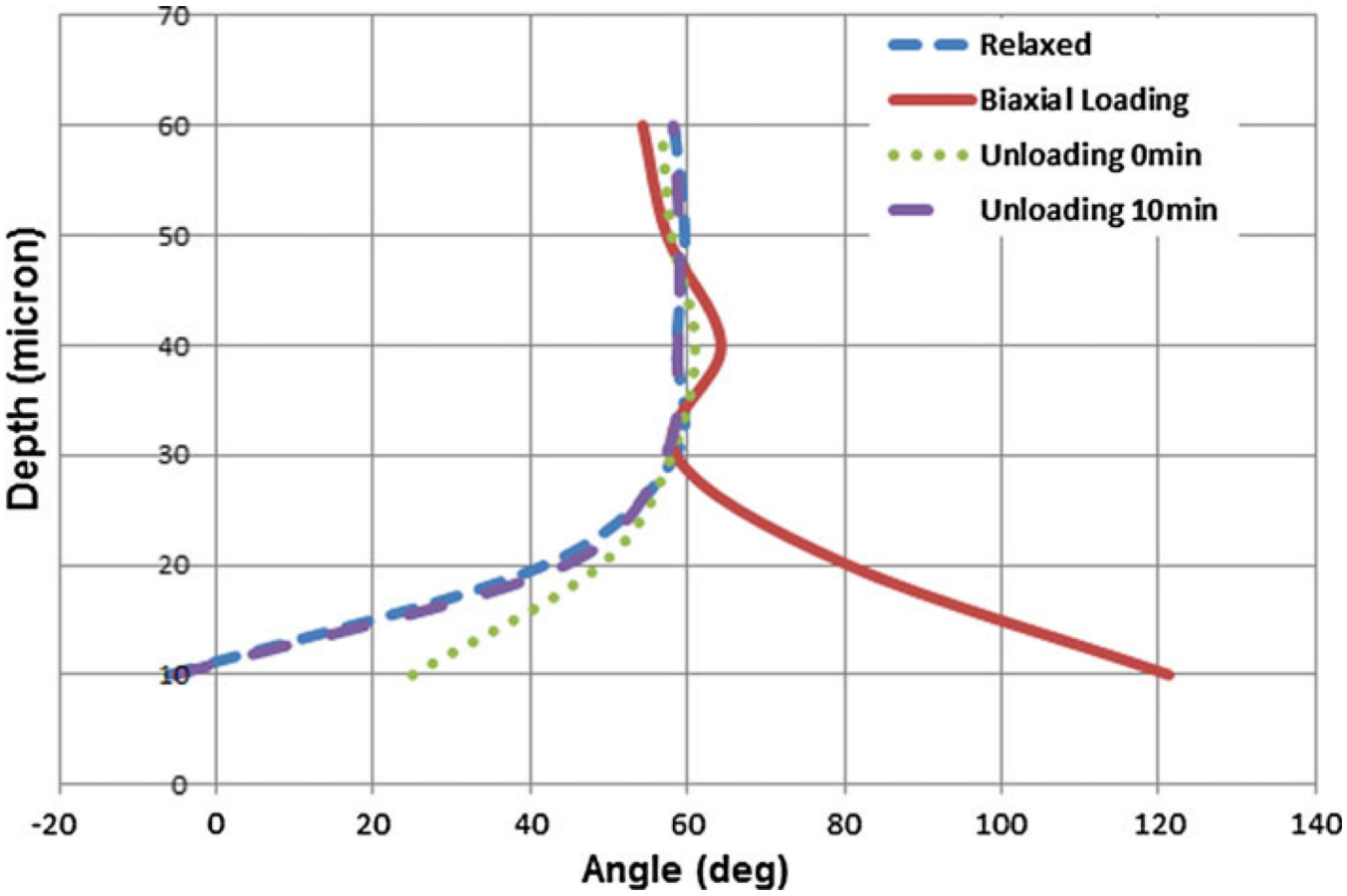

FIGURE 9.

Comparison of collagen fiber orientation in relaxed, loaded and unloaded (right after loading and 10 min after loading) states of the first bovine pericardial sheet. Biaxial loading state shows that fibers arrange almost at 60° angle in deeper layers while they are almost at 120° at the surface.

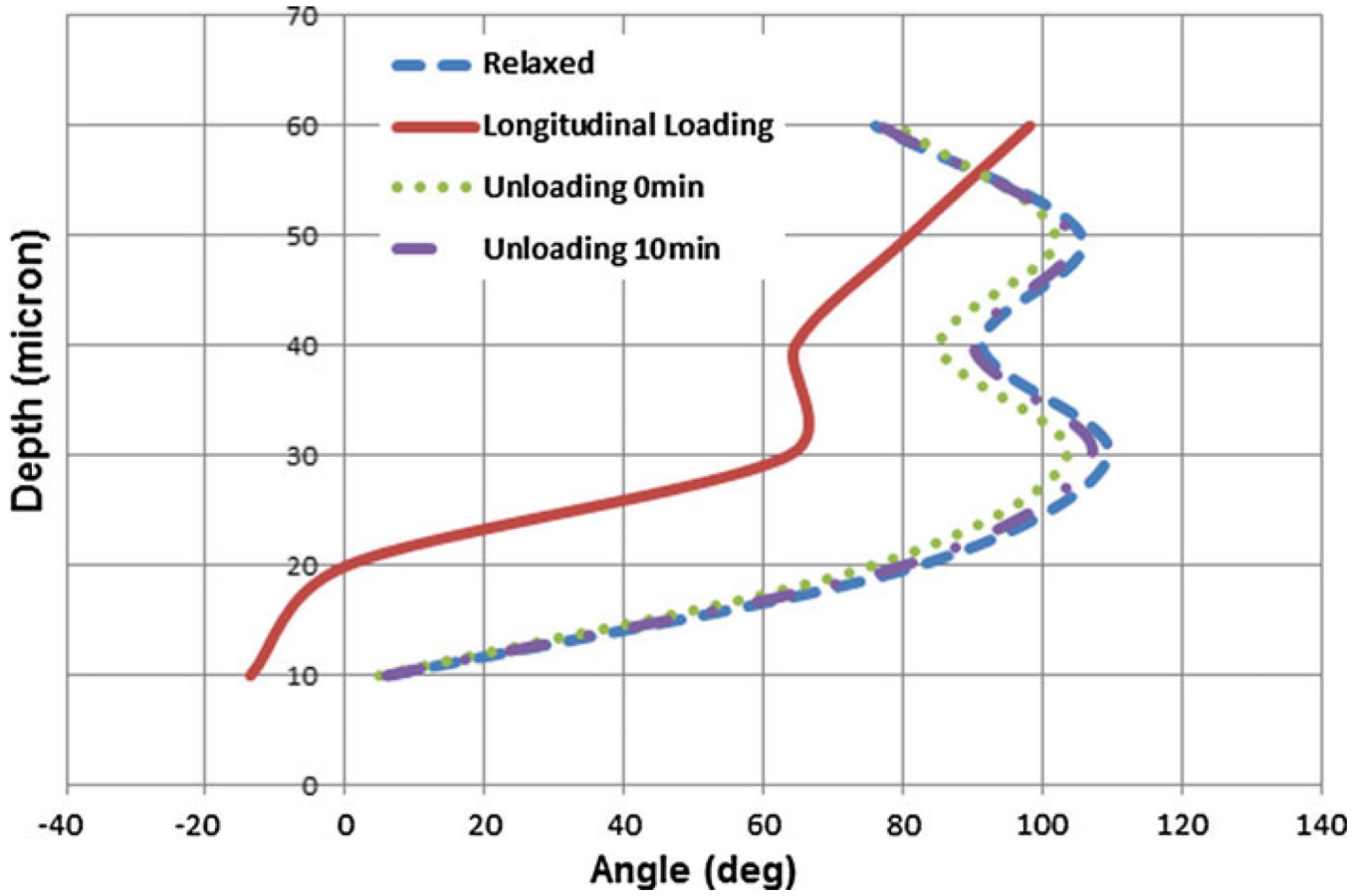

FIGURE 10.

Comparison of collagen fiber orientation in relaxed, loaded and unloaded (right after loading and 10 min after loading) states of the second bovine pericardial sheet. Uniaxial longitudinal loading state shows that fibers are almost perpendicular to force at the surface and in-line with the force in deeper layers. The relaxed state shows quite different fiber orientation with respect to the first sample.

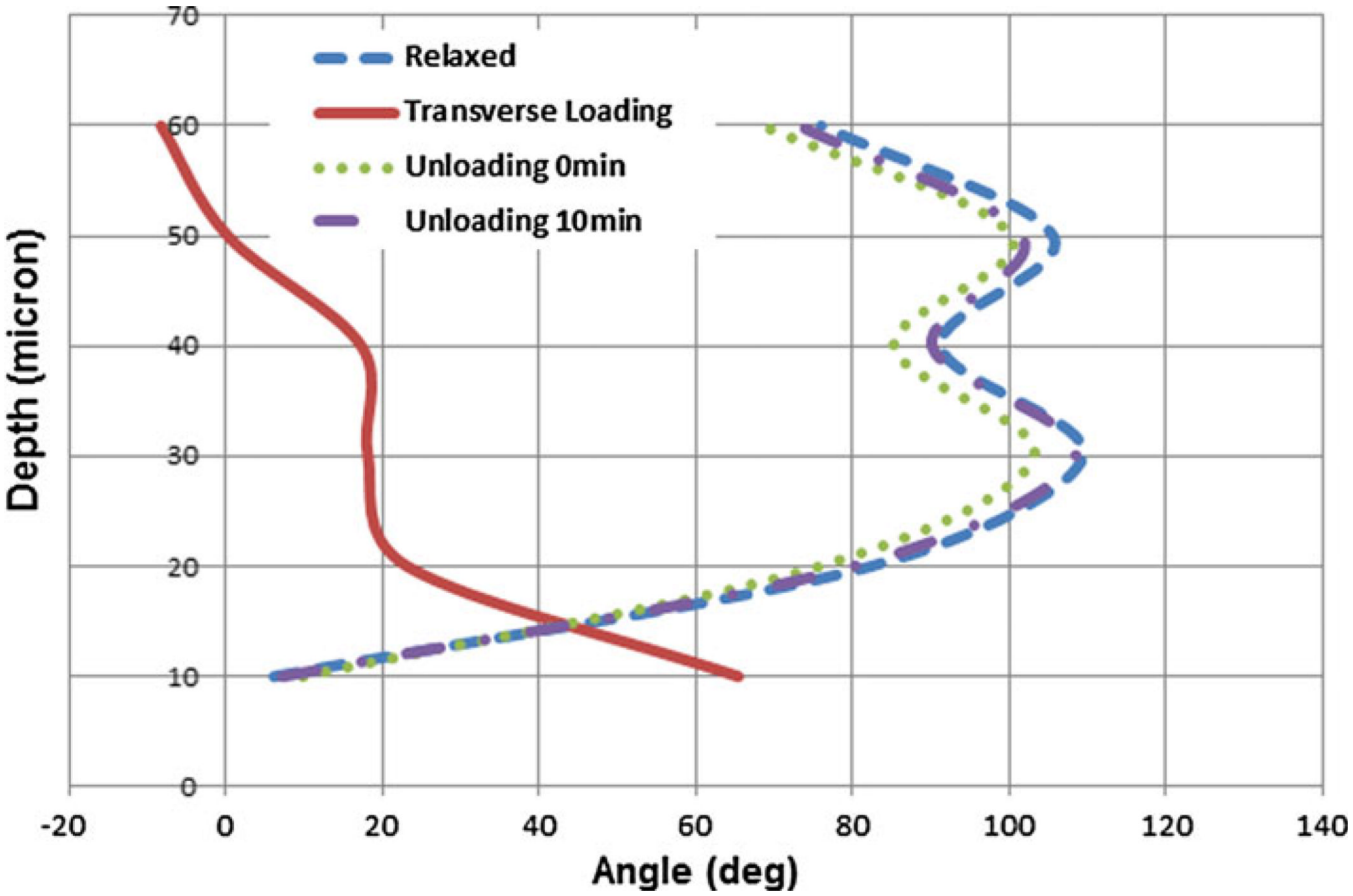

FIGURE 11.
Comparison of collagen fiber orientation in relaxed, loaded and unloaded (right after loading and 10 min after loading) states of the second bovine pericardial sheet. Uniaxial transverse loading state shows that the fibers are in-line with the load at deeper layers.

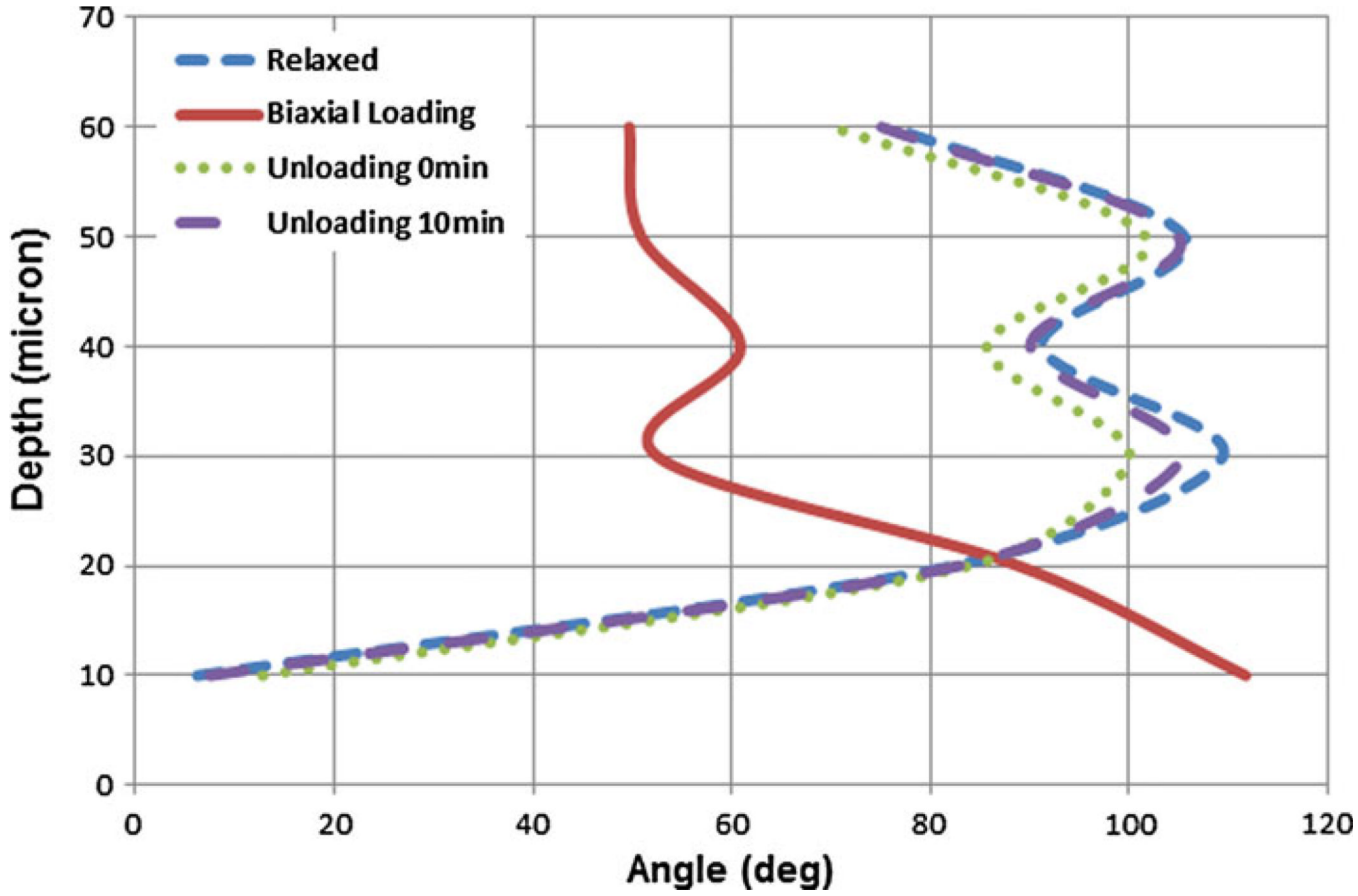

FIGURE 12.
Comparison of collagen fiber orientation in relaxed, loaded and unloaded (right after loading and 10 min after loading) states of the second bovine pericardial sheet. Biaxial loading state shows that fibers arrange almost at 50° angle in deeper layers while they are almost at 120° at the surface.

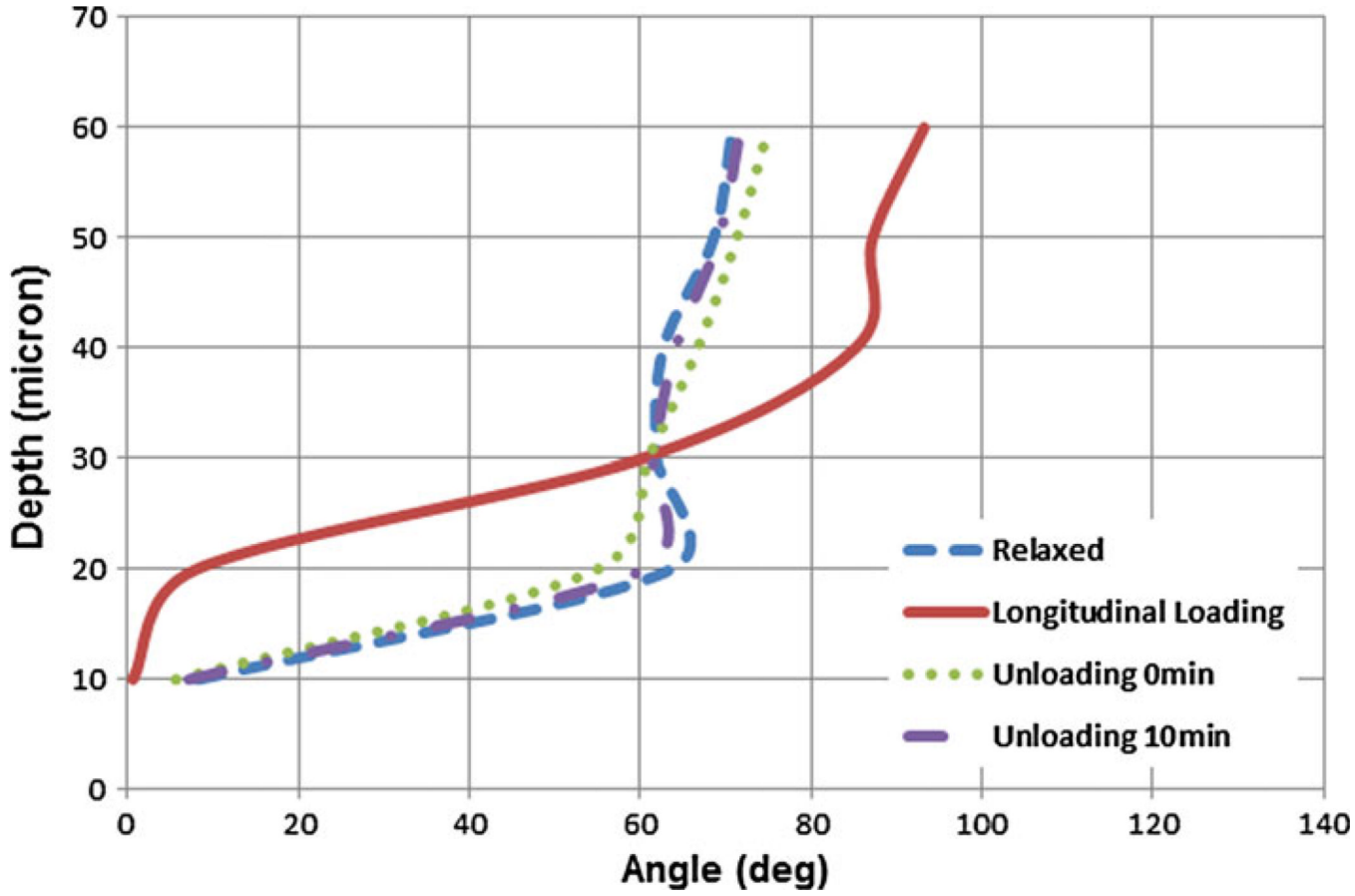

FIGURE 13.

Comparison of collagen fiber orientation in relaxed, loaded and unloaded (right after loading and 10 min after loading) states of the third bovine pericardial sheet. Uniaxial longitudinal loading state shows that fibers are almost perpendicular to force at the surface and in-line with the force in deeper layers. The relaxed state shows quite different fiber orientation with respect to the first and second samples.

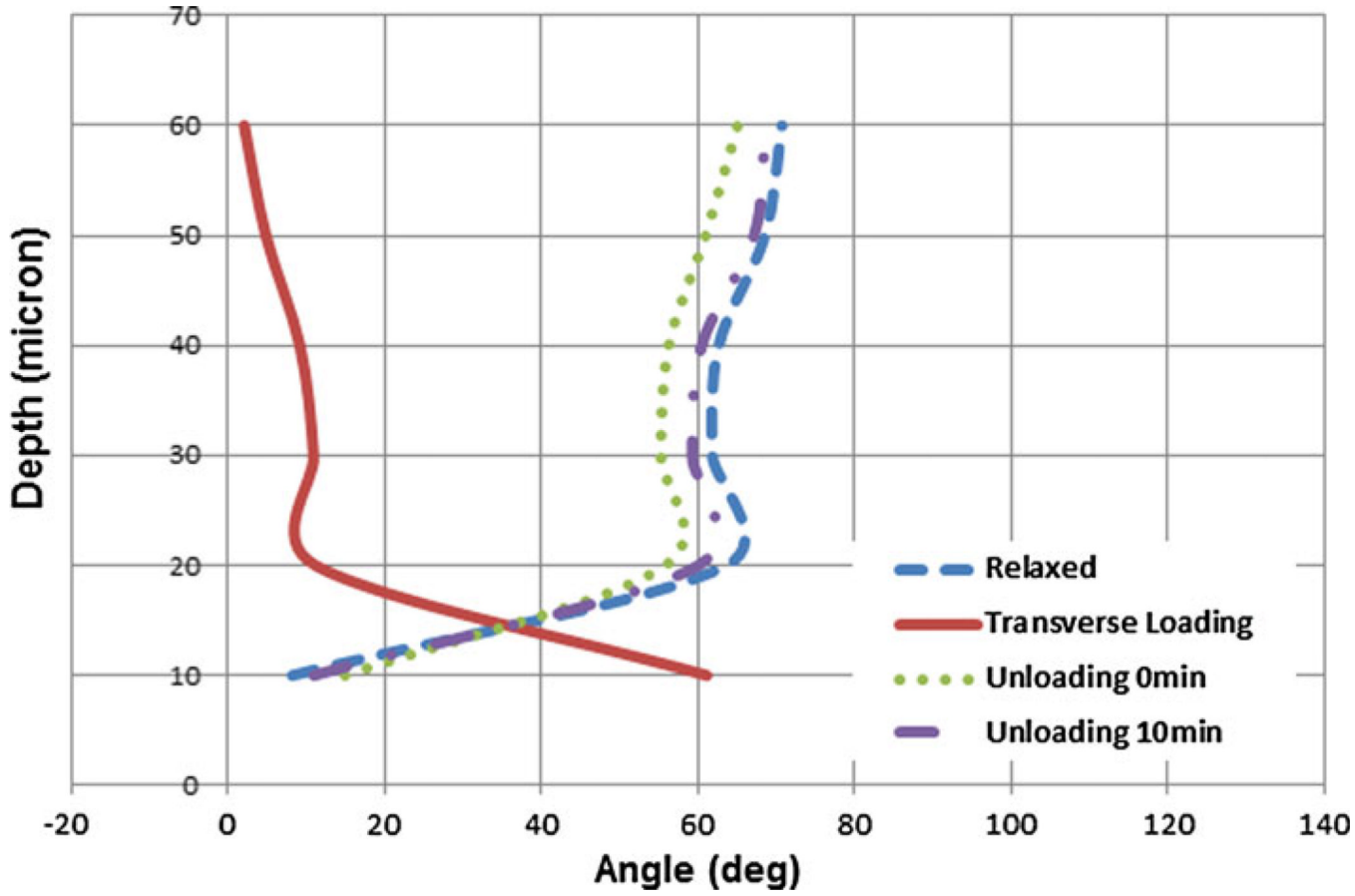

FIGURE 14.

Comparison of collagen fiber orientation in relaxed, loaded and unloaded (right after loading and 10 min after loading) states of the third bovine pericardial sheet. Uniaxial transverse loading state shows that the fibers are in-line with the load at deeper layers and almost at 60° at the surface.

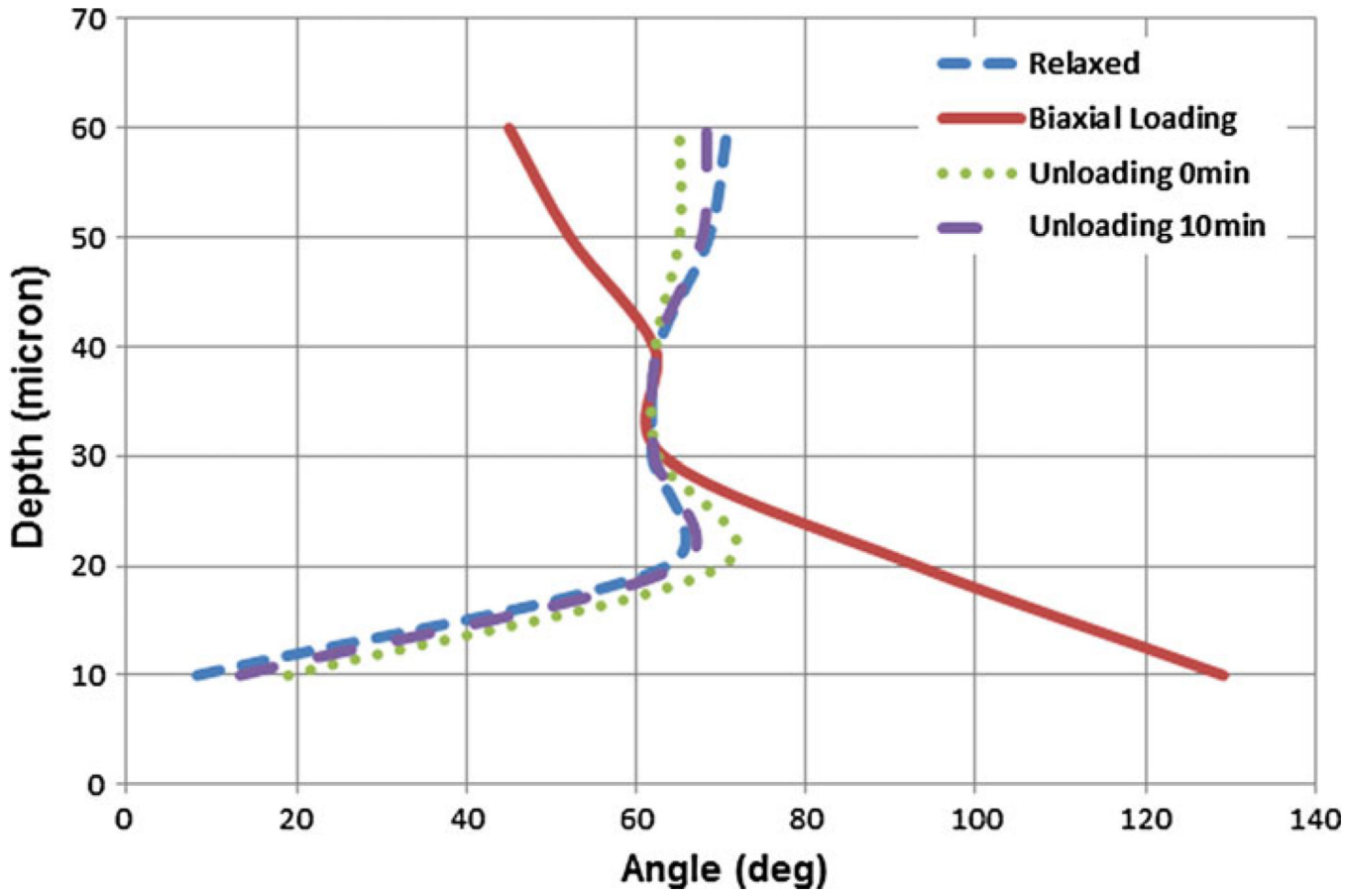

FIGURE 15.
Comparison of collagen fiber orientation in relaxed, loaded and unloaded (right after loading and 10 min after loading) states of the third bovine pericardial sheet. Biaxial loading state shows that fibers arrange almost at 45° angle in deeper layers while they are almost at 130° at the surface.

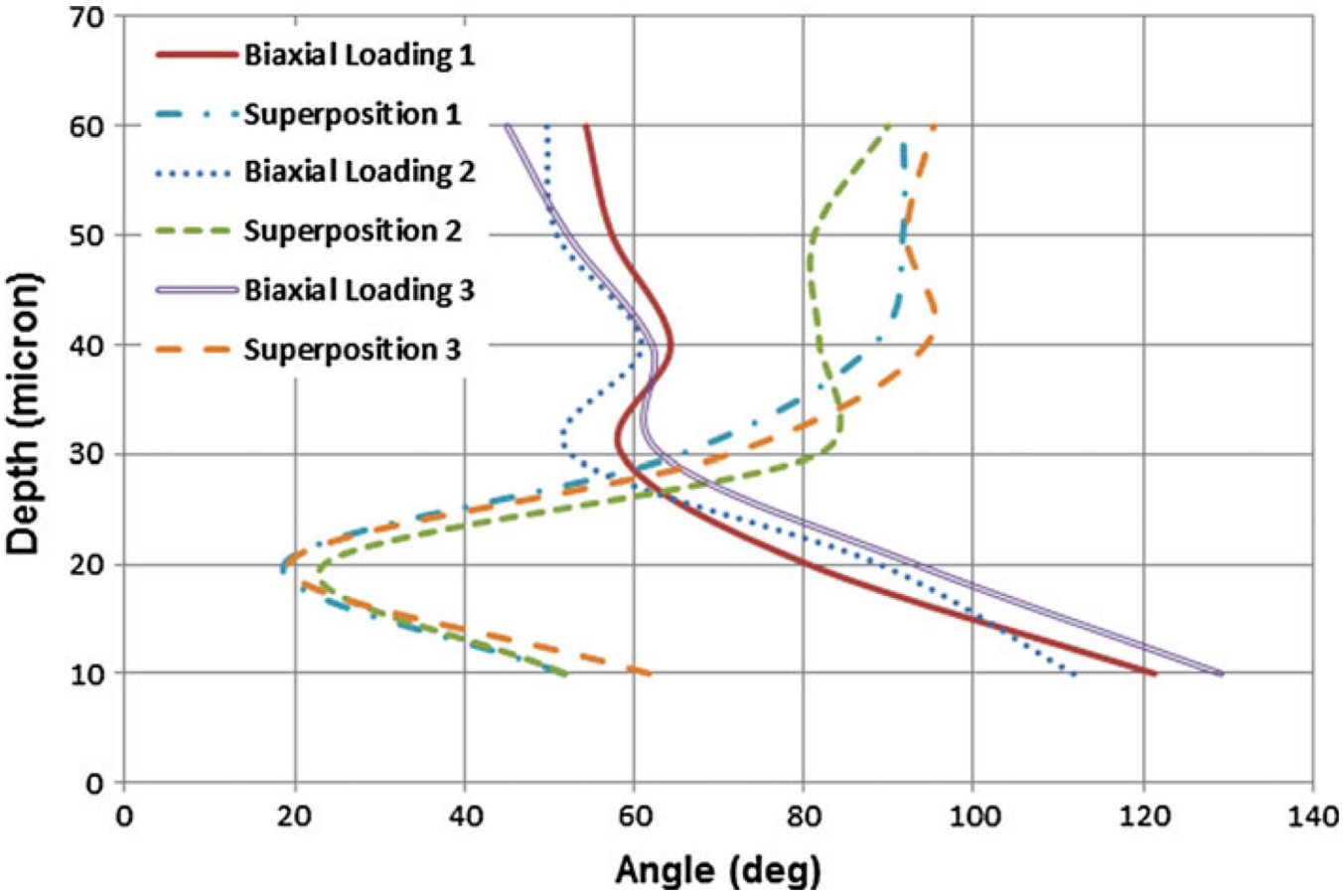

FIGURE 16.
Comparison of collagen fiber orientation in biaxially loaded vs. superposition of uniaxially loaded (longitudinal plus transverse) states of all bovine pericardial sheet samples. The graphs show that the biaxial behavior is totally different from uniaxial superposed data for all samples.